

Article

Not peer-reviewed version

---

# Hydrogen Permeability of Composite Pd-Au/Pd-Cu Membranes and Methods for Their Preparation

---

Polina Pushankina , Georgy Andreev , [Iliya Petriev](#) \*

Posted Date: 29 June 2023

doi: [10.20944/preprints202306.2141.v1](https://doi.org/10.20944/preprints202306.2141.v1)

Keywords: membrane technologies; palladium-containing films; surface modification; nanostructured surface; pentagonal structured particles; catalytic activity; hydrogen permeability; hydrogen carriers; high-purity hydrogen



Preprints.org is a free multidiscipline platform providing preprint service that is dedicated to making early versions of research outputs permanently available and citable. Preprints posted at Preprints.org appear in Web of Science, Crossref, Google Scholar, Scilit, Europe PMC.

Copyright: This is an open access article distributed under the Creative Commons Attribution License which permits unrestricted use, distribution, and reproduction in any medium, provided the original work is properly cited.

Article

# Hydrogen Permeability of Composite Pd-Au/Pd-Cu Membranes and Methods for Their Preparation

Polina Pushankina <sup>1</sup>, Georgy Andreev <sup>1</sup> and Iliya Petriev <sup>1,2,\*</sup>

<sup>1</sup> Department of Physics, Kuban State University, Krasnodar 350040, Russia

<sup>2</sup> Laboratory of Problems of Stable Isotope Spreading in Living Systems, Southern Scientific Centre of the RAS, Rostov-on-Don 344006, Russia

\* Correspondence: petriev\_iliiya@mail.ru

**Abstract:** Thin Pd-40%Cu films were obtained by the classical melting and rolling method, magnetron sputtering and modified with nanostructured functional coatings to intensify the process of hydrogen transport. The films were modified by electrodeposition according to the classical method of obtaining palladium black and "Pd-Au nanoflowers" with spherical and pentagonal particles, respectively. The experiment results demonstrated the highest catalytic activity ( $89.47 \text{ mA cm}^{-2}$ ), good resistance to CO poisoning and long-term stability of Pd-40%Cu films with a pentagonal structured coating. The investigation of the developed membranes in the hydrogen transport processes in the temperature range of 25–300°C also demonstrated high and stable fluxes up to  $475.28 \text{ mmol s}^{-1} \text{ m}^{-2}$  (deposited membranes) and  $59.41 \text{ mmol s}^{-1} \text{ m}^{-2}$  (dense-metal membranes), which turned out to be up to 1.5 higher compared to membrane materials with classic niello. For all-metal modified membranes, the increase in flux was up to 7 times, compared with a smooth membrane made of pure palladium, and for deposited films, this difference was several tens of times. The membrane materials selectivity was also high up to 4419. The developed strategy for modifying membrane materials with functional coatings of a fundamentally new complex geometry can shed new light on the development and fabrication of durable and highly selective palladium-based membranes for gas steam reformers.

**Keywords:** membrane technologies; palladium-containing films; surface modification; nanostructured surface; pentagonal structured particles; catalytic activity; hydrogen permeability; hydrogen carriers; high-purity hydrogen

## 1. Introduction

The rapidly developing hydrogen energy and high-tech industries are increasingly encouraging the development of hydrogen generation technologies. Nowadays, the most popular and effective technology for high-purity hydrogen evolution is the membrane separation. Over the past few decades, membrane technology has been developed and investigated to meet various requirements of different applications [1–7]. It has a number of advantages, such as low energy consumption, the ability to conduct continuous separation, easy scaling and the ability to combine with other separation technologies [8,9]. Palladium membranes are most preferred in the industrial hydrogen separation conditions. [10–12]. Such phenomena is due to the high ability of palladium to transport hydrogen in a wide temperature range due to the higher solubility and diffusion ability of the FCC lattice. However, the practical application of membranes based on pure palladium is limited, since the metal tends to embrittlement in a hydrogen atmosphere [13,14]. Therefore, the membranes usage for hydrogen separation is very difficult and sometimes even impossible due to lattice expansion caused by dissolved hydrogen at temperatures below 300 °C [15,16]. This fact is due to the two immiscible Pd  $\alpha$ - and  $\beta$ -phases, the first of which is a solid solution, and the second one is palladium hydride [17,18]. There is a transition between the  $\alpha$ - and  $\beta$ -phases with the lattice space increase up to 10%. It leads to a lattice distortion, the high internal stresses formation, deformation, and,

ultimately, the membrane destruction [19]. In addition to embrittlement, palladium is quite susceptible to poisoning and surface contamination by impurity gases, which contain sulfur or carbon compounds [20–22]. Also, a significant difficulty in the fabrication of membranes based on pure palladium is the high metal cost [23,24]. Alloying of palladium with other metals, such as silver, gold, copper, ruthenium, nickel, makes it possible to overcome these difficulties [25–28]. For example, Q. Zhou et al. have studied gas separation properties of membranes based on Pd-Au and Pd-Au-Ag alloys [29]. The obtained results demonstrated the lowest hydrogen gas adsorption energy of -0.017 eV and -0.010 eV for Pd-Au and Pd-Au-Ag and excellent hydrogen selectivity and permeability characteristics of the developed membranes. Z. Han et al. [30] have investigated the characteristics of hydrogen separation by Pd-based alloy membranes using the density functional theory (DFT) modeling and molecular dynamics calculations. According to the results, the Pd-Cu and Pd-Ni membranes showed excellent hydrogen selectivity compared to nitrogen, carbon monoxide, carbon dioxide, methane, hydrogen sulfide at various temperatures, and the hydrogen permeability exceeded the limits of industrial production. S. Agnolin et al. [31] described the fabrication of thin Pd-Ag membranes on Hastelloy X tubular filters. A thin membrane layer was deposited on the surface of a tube modified by polishing and applying a smoothing interdiffusion barrier layer based on a boehmite dispersion. The filter pre-treatment was critical to increase the permeability and hydrogen selectivity of the final membrane in fact.

One of the most promising membrane systems is the Pd-Cu binary alloy, which has good mechanical properties, high thermal stability, excellent hydrogen selectivity and permeability, relatively low cost, resistances to hydrogen sulfide poisoning, prevents hydrogen embrittlement at low temperatures [32–34]. According to the phase diagram [35,36], Pd-Cu alloys mainly have two different crystal lattices: face-centered cubic (fcc) and body-centered cubic (bcc) [37,38]. The most attractive for the membrane alloys manufacture is the bcc structure, since such Pd-Cu alloys demonstrate the highest hydrogen permeability compared to the fcc structure ones [39–41]. Pd-40%Cu with a bcc structure and the highest hydrogen permeability seems to be especially promising of the variety of known alloys [42,43].

Another important factor in improving the Pd-based membranes efficiency and durability is the membrane film thinning. The deposition of a thin film on porous supports allows to increase the hydrogen penetration rate and to reduce the cost of the material compared to the traditional Pd dense-metal membranes [44–46]. Nowadays, the most common methods for manufacturing such a composite membrane are vacuum deposition, chemical-vapor deposition, chemical and galvanic deposition [47–49]. Among these methods, magnetron sputtering has a clear advantage, since it provides the synthesis of ultrathin films with a minimum impurities, greater flexibility in the alloy synthesis, ease of control of process parameters, and the possibility of creating a nanostructured film [50,51].

However, another significant problem of hydrogen membrane separation today is the extremely small and unstable or non-existent permeability of palladium-containing membranes at low temperatures (less than 200 °C). This fact is caused by the kinetic inhibition of establishing the equilibrium of metal-hydrogen systems, which is mainly due to an inactive or contaminated metal surface [52]. In this case, surface processes limit the hydrogen transport. The limit, which slows down the establishment of equilibrium between molecular hydrogen in the gas phase and atomic hydrogen absorbed in the palladium phase, can be partially overcome by increasing the surface roughness coefficient. "Catalytically active" cracks facilitates the establishment of equilibrium with hydrogen gas. They occur during alternating electrolytic oxidation and reduction, prolonged exposure to a glow discharge or calcination in air. So N. Vicinanza et al. [53] subjected Pd77%Ag23% membranes to a three-stage air heat treatment to investigate the positive effects of such treatment on hydrogen transfer. It was found that air heat treatment affects the roughness and increases the effective membrane surface area, which increases the hydrogen permeability after each of the stages. In particular, surface activation can be carried out by applying a "hydrogen carriers" coating (modifier). There are various methods such as the reduction of metal ions in solution, growth in the gas phase, evaporation on a substrate, electrochemical deposition, which are promising for obtaining modifying

coatings. "Hydrogen carriers" are hydrogen chemisorbing substances such as platinum metals [54]. The nanostructured palladium layer formation on the membrane surface will increase the actual working surface area, thus lead to an increase in the chemisorption centers number [55,56]. The deposition of a modifier based on pentagonal structured multiply twinned nanoparticles is particular interesting and effective. Membranes modified with such a coating make it possible to increase hydrogen permeability by several times in the low-temperature operating range [57,58]. The novelty of the work is to study of the effect of surface modifiers of various morphologies on membrane materials in the low-temperature hydrogen transport.

In according to the foregoing, the aim of this work was to intensify the process of low-temperature hydrogen permeability of palladium-copper membranes by modifying the surface with a nanostructured coating, which is pentagonal multiply twinned palladium-gold particles.

## 2. Materials and Methods

### 2.1. Methods for Creating and Studying Membrane Materials

Thin films of the Pd-40%Cu alloy were obtained by three methods:

The first method was to obtain a homogeneous Pd-Cu alloy by melting the constituent metal components of palladium and copper in an electric arc furnace in an inert argon atmosphere. Metals in the form of Pd ingots and oxygen-free copper were get to a copper crucible for melting. The pressure inside the chamber was 0.05 MPa. In the melting process, the inverter current was increasing from 30 to 90 A. Next, the obtained Pd-40%Cu ingot was rolled out on rollers to a film thickness of 20  $\mu\text{m}$  with intermediate annealings.

The second method consisted in obtaining dense defect-free films of the Pd-Cu alloy with thickness up to 300 nm on a hydrogen-permeable substrate from an aluminium oxide by magnetron sputtering from a continuous Pd-40%Cu target. The target was obtained by the first method by alloying components and rolling up to 40  $\mu\text{m}$  with intermediate annealing. The films were deposited at a current of 40–50 mA on both sides of the substrate.

The third method for obtaining Pd-40%Cu on the base surface completely repeats the previous one. However, the main difference between the third method and the second one is the usage of a composite target consisting of palladium and copper plates with an area ratio of 60:40. The main advantage of this method is easily changing of the elements percentage in the alloy without the melting procedure and any changes in the resulting alloy structure.

The obtained films phase composition was determined on a Shimadzu XRD-7000 X-ray diffractometer. The samples were studied in the range of 2 $\theta$  angles from 30° to 80° with a scanning step of 0.02° using CuK $\alpha$  radiation ( $\lambda = 1.5406 \text{ \AA}$ ) at a current of 30 mA and an accelerating voltage of 40 kV.

### 2.2. Synthesis and Study of the Morphology of Nanostructured Coatings

Modification of the developed Pd-40%Cu alloy films was carried out by two methods:

The first method – classical palladium black – was carried out using electrochemical deposition from a palladium chloride solution using a potentiostat-galvanostat Elins P-40X. Palladium-copper films were preliminarily prepared by washing and degreasing, after which samples were fixed in an electrolytic cell for polarization. Anode polarization was carried out in HCl at a current density of 10 mA  $\text{cm}^{-2}$ , then cathodic polarization was carried out in H<sub>2</sub>SO<sub>4</sub> at the same current. After pretreatment, the cell with prepared electrodes was filled with a palladium chloride solution. Deposition was carried out at a current density of 6 mA  $\text{cm}^{-2}$  on both sides of the films.

The second method – Pd-Au nanoflowers – was based on the classical palladium black method; so the synthesis was carried out according to a similar algorithm. A significant difference from the previous method was the synthesis process itself. The prepared electrodes were placed in a working cell filled with a growth solution of palladium chloride with a surfactant tetrabutylammonium bromide. Electrodeposition was carried out from a palladium-gold alloy electrode at a current density of 3 mA  $\text{cm}^{-2}$  on both sides of the films to obtain palladium-gold particles.

The samples surface morphology was investigated by a JEOL JSM-7500F scanning electron microscope.

### 2.3. Study of Developed Materials in Catalytic and Membrane Applications

Cyclic voltammetry (CV) in the alkaline methanol oxidation reaction in the potential range from -0.9 to + 0.5 V at a scanning rate of 50 mV s<sup>-1</sup> investigated the catalytic activity of the modified films. The composition of the working solution is 1 M NaOH + 0.5 M methanol. The measurements were carried out on a P-40X potentiostat-galvanostat in a three-electrode cell: the working electrode was each sample of modified Pd-40%Cu films, the counter electrode was a platinum electrode, and the reference electrode was a silver chloride glass electrode (Ag/AgCl), relative to which the potentials were reported.

The long-term stability of the developed nanoparticles as catalysts was studied by chronoamperometry in the reaction of alkaline methanol oxidation at a constant potential of -0.3 V during 0–2400 s.

The study of the hydrogen transfer processes through the developed samples of membrane materials was carried out by the special measuring hydrogen permeability device according to the method described in the work [59].

## 3. Results and Discussion

### 3.1. Structural Characteristics of the Developed Membrane Materials

Membrane materials obtained by three methods at the work were characterized using the XRD method. The obtained X-ray diffraction spectra of Pd-40%Cu alloy films obtained by melting and classical rolling (M<sub>1</sub>), magnetron sputtering from a solid target (M<sub>2</sub>) and a composite target (M<sub>3</sub>) are shown in Figure 1. The face-centered cubic crystal structure (fcc) of palladium is characterized by four peaks at 2θ values equal to 40.1, 46.7, 68.2 and 82.2 corresponding to the planes (111), (200), (220) and (311) respectively. The crystal copper structures was characterized by four peaks at 2θ values equal to 43.3, 50.4, 74.1, and 89.9 [60]. Analyze of the X-ray diffraction patterns of the samples shown in Figure 1 demonstrate appearance of each diffraction peak between the corresponding positions of the the Pd and Cu fcc structure peaks, which confirms the successful formation of the Pd-Cu alloy.

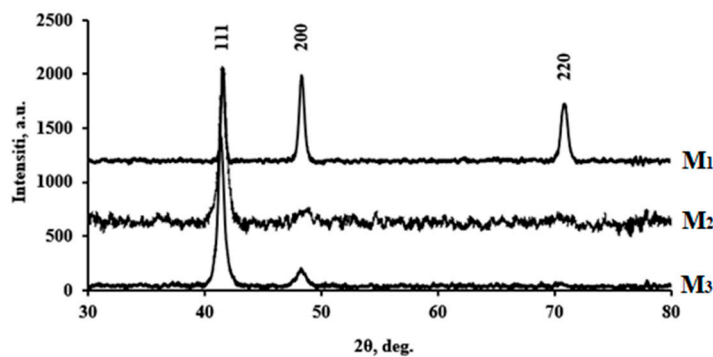


**Figure 1.** X-ray diffraction spectra of Pd-40%Cu alloy films.

As is known [61], diffraction peaks are shifted to higher values of 2θ due to a lattice constant decrease, which is associated with a smaller diameter of copper atoms compared to palladium ones. The studied samples 2θ values were 41.6, 48.3, and 70.9, corresponding to the (111), (200), and (220) planes, respectively. The lattice parameters (*a*) for bulk palladium and copper are 3.891 Å and 3.615 Å, respectively [62]. The lattice parameters for the studied samples and literary analogues are given in Table 1. The obtained data also confirm the formation of a single fcc structure. The sizes of crystallites (*D*) (regions of coherent scattering) were also calculated using the Scherrer formula (Table 1). Data analysis leads to conclude that the samples obtained by two methods of magnetron

sputtering are characterized by a smaller crystallite size, compared with the samples obtained by alloy and rolled products.

**Table 1.** Parameters of the studied Pd-40%Cu films and literary analogues.

Film	Elemental composition		a, Å	D, nm	Reference
Pd-Cu M <sub>1</sub>	Pd	60.08	3.76±0.002	30.5	This work
	Cu	39.92			
Pd-Cu M <sub>2</sub>	Pd	59.96	3.76±0.06	21.1	This work
	Cu	40.04			
Pd-Cu M <sub>3</sub>	Pd	60.31	3.77±0.003	22.1	This work
	Cu	39.69			
Pd-Cu	Pd	50	3.77	–	[11]
	Cu	50			
Pd-Cu	Pd	55.31	3.867	–	[17]
	Cu	44.69			
Pd-Cu	Pd	53.1±0.4	3.775	–	[36]
	Cu	46.9±0.4			
Pd-Cu	Pd	51.9±0.4	3.763	–	[38]
	Cu	48.1±0.4			
Pd-Cu	Pd	46	3.782	–	[47]
	Cu	54			
Pd-Cu	Pd	59.2±0.8	3.757±0.003	–	[63]
	Cu	40.8±0.8			

Pd-40%Cu film obtained by alloying components and rolling had a fairly smooth surface. SEM images of the Pd-40%Cu membrane surfaces studied in the work are shown in Figure 2.

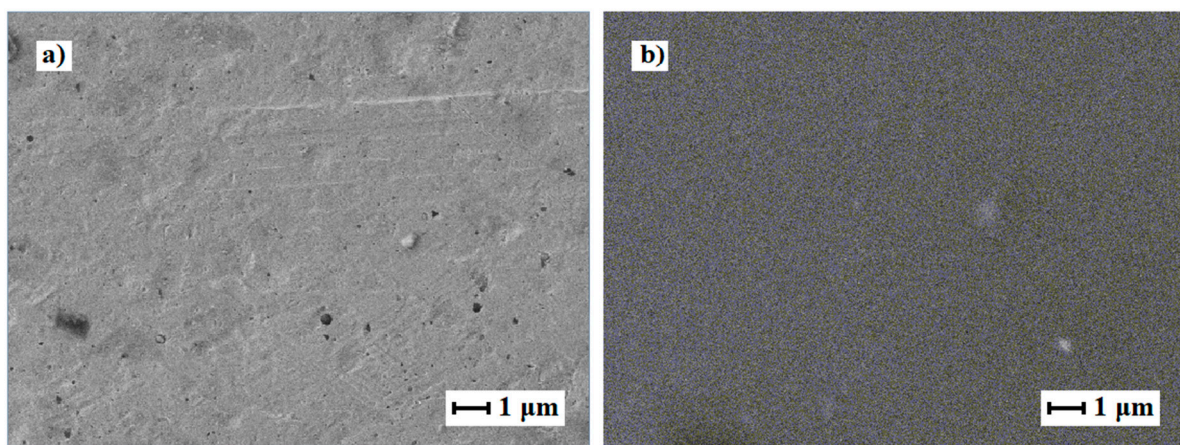


**Figure 2.** SEM images of the Pd-40%Cu membrane obtained by alloying components and rolling and by magnetron sputtering.

## 2.2. Morphology of Nanostructured Coatings and Catalytic Characteristics of Modified Films

The nanostructured coating on the Pd-40%Cu alloy film surfaces of synthesized by the method of classical palladium black consisted of typical spherical particles with characteristic sizes in the range of 90–120 nm. SEM images of the surface of films modified by the classical palladium black method are shown in Figure 3. After applying the modifier on the Pd-40%Cu films surface, the real working surface area increased up to 9.4 times and the coating roughness coefficient increased to 15.13.

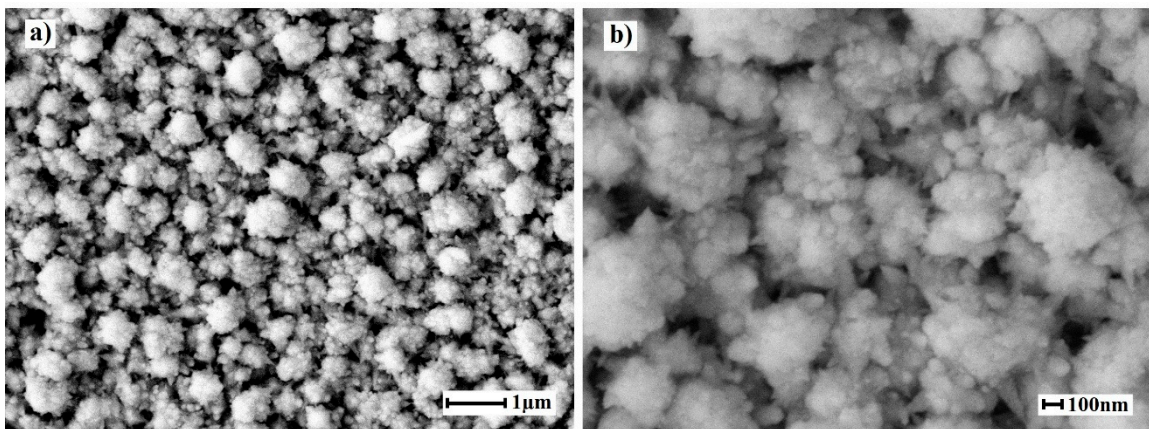


**Figure 3.** SEM images of the surface of Pd-40%Cu films modified by the classical palladium black method.

The nanostructured coating on the of Pd-40%Cu alloy films surfaces synthesized by the “nanoflowers” method consisted of pentagonal structured Pd-Au nanoparticles with multiple corrugations with characteristic sizes in the range of 100–130 nm. To obtain such coatings with a large number of active centers, the particles growth was directed towards high-index facets. SEM images of the surface of the films modified by the “Pd-Au nanoflowers” method are shown in Figure 4. After applying the modifier on the Pd-40%Cu films surface, the real working surface area increased up to 11.2 times and the coating roughness coefficient increased to 18.02.

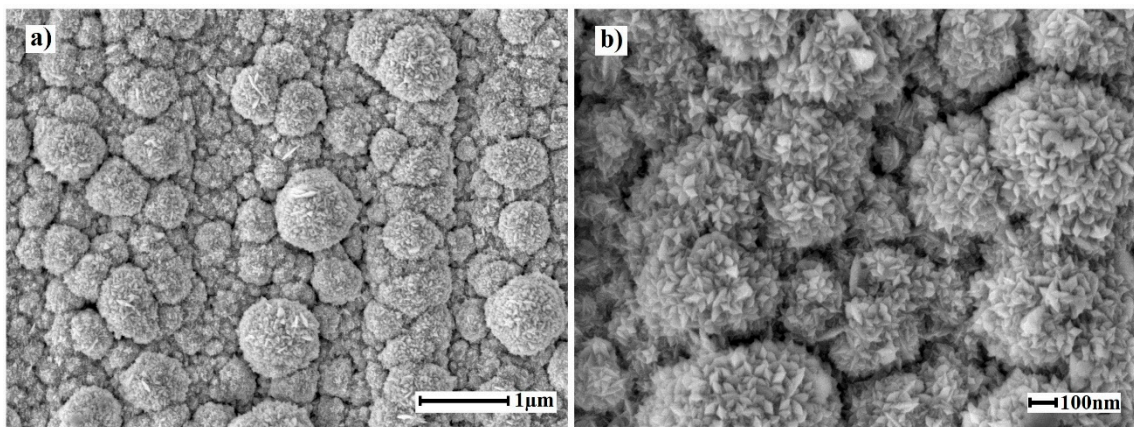


**Figure 4.** SEM images of the surface of Pd-40%Cu films modified by the “Pd-Au nanoflowers” method.

The average thickness of the modifying layer was about 0.7  $\mu\text{m}$ . SEM images of cross-sections of modified samples of Pd-40%Cu films obtained by alloying and rolling and magnetron sputtering are shown in Figure 5.

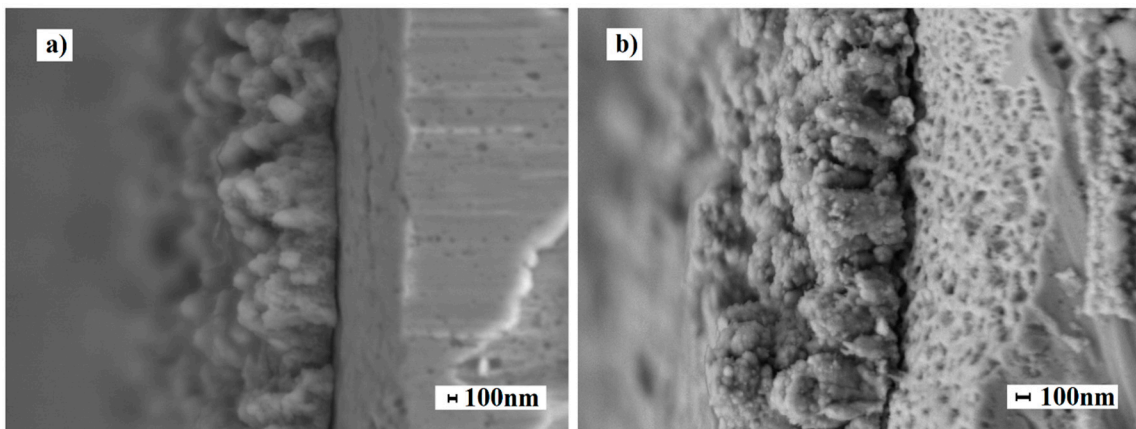


**Figure 5.** SEM images of cross-sections of modified samples of Pd-40%Cu films obtained by alloying and rolling (a) and magnetron sputtering (b).

The developed of Pd-40%Cu M<sub>1</sub> film samples modified with two types of coatings pentagonally structured (Pd-Au) и classic black (Pd<sub>black</sub>) were studied in the alkaline methanol oxidation reactions. As it shown in Figure 6, two peaks can be observed on all current-voltage curves in the potential range from -1 to 0.5 V. The oxidation peak in the forward scan is related to the chemisorbed methanol electrooxidation, and the oxidation peak in the reverse one is associated with the removal of carbonaceous intermediates that were not completely oxidized in the forward scan. The data demonstrate a significant increase up to 89.47 mA cm<sup>-2</sup> in the peak current density of Pd-Au/M<sub>1</sub> samples. These peak current density values are up to 2 times higher than the ones for Pd<sub>black</sub>/M<sub>1</sub> films (up to 40.38 mA cm<sup>-2</sup>), and up to several tens of times than unmodified M<sub>1</sub> film values (up to 0.17 mA cm<sup>-2</sup>). Another important activity characteristic of the electrodes in relation to the methanol oxidation reaction is the peak potential shift. With a further increase in the potential, the current density begins to decrease due to an increase in the coverage of CO<sub>ads</sub> on the active centers and depletion of methanol near to the electrode surface. It should also be noted that the synergistic effect of bimetallic compositions of palladium with gold plays one of the key roles in the catalytic activity increase. This combination makes it possible to most effectively inhibit the poisoning of palladium active sites due to the ability of gold to accelerate the oxidation of intermediate reaction products [64].

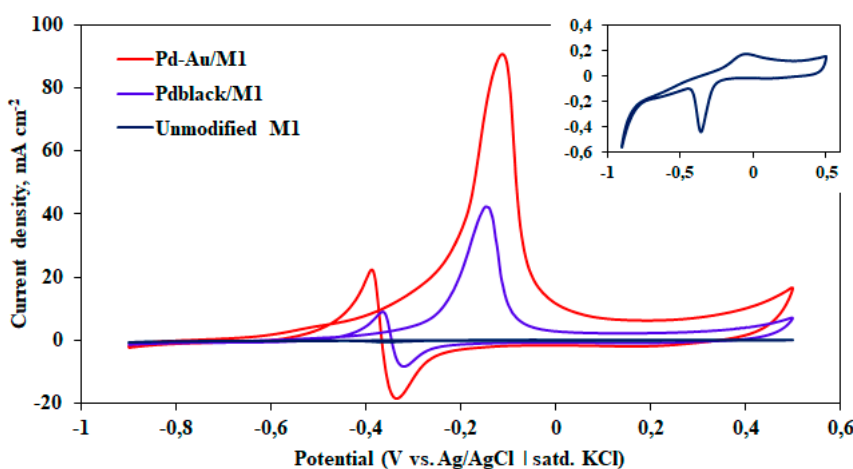


**Figure 6.** Established CV of Pd-40%Cu films.

The catalysts resistance to CO poisoning was evaluated in terms of the ratio of the current peaks appearing during the forward and reverse scans [65]. High values of the ratio indicate effective desorption of CO on the developed modified electrodes, and on the contrary, low values indicate an

excessive accumulation of residual  $\text{CO}_{\text{ads}}$  forms on the surface. The highest stability index was demonstrated by  $\text{Pd-Au/M}_1$  samples – 4.5.  $\text{Pd}_{\text{black}}/\text{M}_1$  samples also showed quite good stability – 4.

Another critical aim in the design and development of efficient catalyst systems is to solve stability problems caused by rapid carbonaceous intermediates absorption [66]. The catalysts durability and electrochemical stability were studied by chronoamperometry (CA) at a constant oxidation potential of  $-0.3$  V. Figure 7 shows the measured durability curves of  $\text{Pd-Au/M}_1$  and  $\text{Pd}_{\text{black}}/\text{M}_1$  samples. As it can be seen at Figure 7, a sharp current decrease was fixed in the first seconds of measurements for all samples, before its stable value was reached. The current decrease of  $\text{Pd}_{\text{black}}/\text{M}_1$  samples is more pronounced, which is associated with the adsorption of intermediates formed during methanol oxidation reaction. It can be seen from the CA analysis that the  $\text{Pd-Au/M}_1$  sample has a stable higher stationary current density in the methanol oxidation reaction up  $2.23 \text{ mA cm}^{-2}$ , compared to the  $\text{Pd}_{\text{black}}/\text{M}_1$  ( $1.63 \text{ mA cm}^{-2}$ ) and unmodified  $\text{M}_1$  ( $0.01 \text{ mA cm}^{-2}$ ) samples. This result may be due to a small amount or complete absence of adsorbed intermediates on the catalyst surface. Probably, the main reason for the observed higher stability of  $\text{Pd-Au/M}_1$  samples is the a large number of particles with high-index facets on the surface of Pd-40%Cu films, which lead to the rapid oxidation of adsorbed intermediates with the formation of an active centers large number. The increased stability of the  $\text{Pd-Au/M}_1$  samples is also due to the inclusion of gold, which reduces the CO of electrode surface and increases the electronic conductivity [67]. The current decay is much faster due to the possibility of greater carbon adsorption during the methanol oxidation reaction in the case of  $\text{Pd}_{\text{black}}/\text{M}_1$  samples with pure palladium.

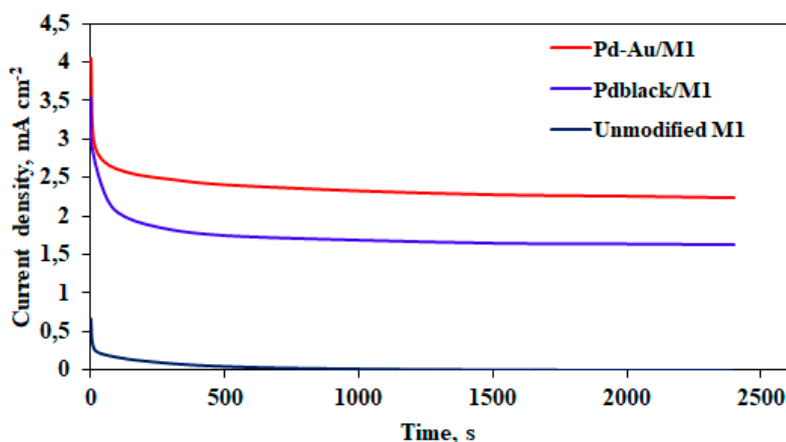


Figure 7. CA curves of methanol oxidation of Pd-40%Cu films.

The study of the developed modifying coatings deposited on Pd-40%Cu films in the methanol oxidation reaction demonstrated a significant increase in the catalytic activity, resistance to CO and stability of  $\text{Pd-Au/M}_1$  films in comparison  $\text{Pd}_{\text{black}}/\text{M}_1$ . The result of the modified films is probably due to an increased number of localized areas of high-energy surface centers, as well as a synergistic effect from the secondary metal (gold) in the composition of the nanoparticles. The formation of active centers in the coating synthesized by the “Pd-Au nanoflowers” method occurs due to multiple twinning of nanoparticles with the high-index facets with a large number of insufficiently coordinated atoms reactive with respect to hydrogen.

### 2.3. Investigation of Modified Membrane Materials in Hydrogen Transport Processes

The synthesized nanoparticles were studied as modifying coatings in hydrogen transport processes. The membrane substrates were Pd-40%Cu  $\text{M}_1$  and  $\text{M}_3$  films. The measurements were carried out in the temperature range from  $25$  to  $300^\circ\text{C}$ , because the effect of the applied modifiers is expected exactly in this range. According to the data presented in Figure 8,  $\text{Pd-Au/M}_1$  and  $\text{Pd-Au/M}_3$  membranes had the highest flux values up to  $59.41 \text{ mmol s}^{-1} \text{ m}^{-2}$  and  $475.28 \text{ mmol s}^{-1} \text{ m}^{-2}$  at  $300^\circ\text{C}$ .

respectively. The  $\text{Pd}_{\text{black}}/\text{M}_1$  and  $\text{Pd}_{\text{black}}/\text{M}_3$  membranes showed a flux 1.5 times less than the previous ones, up to  $307.29 \text{ mmol s}^{-1} \text{ m}^{-2}$  and  $40.97 \text{ mmol s}^{-1} \text{ m}^{-2}$  respectively. The density values of the penetrating fluxes of deposited and dense-metal Pd-40%Cu films obtained by one method and modified by different types of coatings were in the same range, and the difference in the ranges of films obtained by different methods was about 8 times. Such a difference in the flux density is due to the difference in the thickness of the obtained films. This effect can be explained by a significant leveling of the contribution of surface processes to the limitation of hydrogen transfer through palladium-containing membranes.

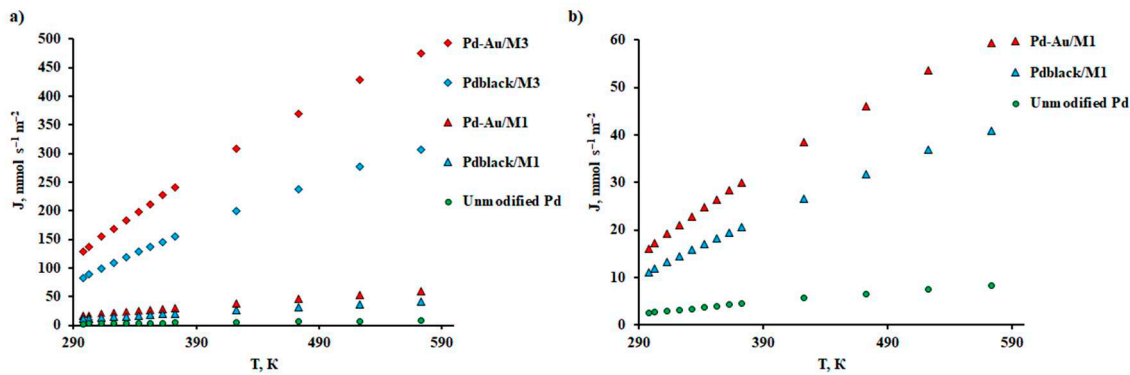


**Figure 8.** a) Temperature dependence of the hydrogen flux at gauge pressure of 0.1 MPa through modified Pd-40%Cu membranes and an unmodified pure palladium membrane. b) Temperature dependence of the hydrogen flux at gauge pressure of 0.1 MPa through modified dense-metal Pd-40%Cu membranes and an unmodified pure palladium membrane.

The achievement of this experiment results became possible due to the limitation of hydrogen transport by dissociative-associative processes on the surface, since the state of the surface has a significant effect in this temperature range (25–300°C). The application of a nanostructured modifier to the membrane sample surfaces lead to an increase in the roughness of the membrane surface as well as an increase in the active centers number. This is especially noticeable for  $\text{Pd-Au/M}_1$  and  $\text{Pd-Au/M}_3$  membranes. The high concentration of such catalytic sites is probably due to the growth features for a given geometric shape of nanoparticles.

The membranes retained their integrity, and the modifying coatings also retained their mechanical integrity without visible changes in the surface condition after experiments in a hydrogen atmosphere. A photo and SEM image of the membrane after experiments to a hydrogen atmosphere are shown in Figure 9.



**Figure 9.** Photo and SEM image of the membrane surface after experiments in a hydrogen atmosphere at gauge pressure of 0.5 MPa in the temperature range of 25–300°C.

The films permeability was also measured depending on the pressure change in the range from 0.1 to 0.5 MPa to determine the limiting stage of hydrogen transport. The experiment was carried out

at a temperature of 100°C, which is of the greatest interest, since it makes it possible to most clearly observe the effect of surface processes on permeability. As it can be seen in Figure 10, the data obtained for an unmodified pure palladium membrane are well approximated by a first-order curve, and the exponent  $n$  is close to 1. This result indicates that the process of hydrogen transfer through a smooth palladium membrane is completely limited by surface effects. In the case of Pdblack/M<sub>1</sub> and Pdblack/M<sub>3</sub> membranes, the exponent  $n$  has the value up to 0.9 and 0.89 respectively, which indicates that the hydrogen transport process is limited by the combination of surface stages and diffusion, but the role of the first ones is still more prevalent. The Pd-Au/M<sub>1</sub> and Pd-Au/M<sub>3</sub> membranes show a more parabolic curve with an  $n$  up to 0.75 and 0.74 respectively. This value are close to 0.5, which indicates a partial removal of surface limits and a greater transition to a diffusion-limited regime.

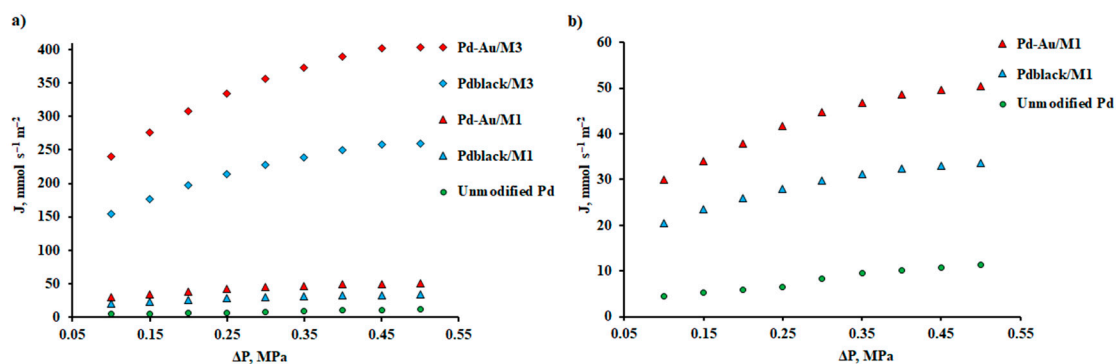


**Figure 10.** a) Dependence of the hydrogen flux on the inlet side gauge pressure at 100°C of modified Pd-40%Cu membranes and an unmodified pure palladium membrane. b) Dependence of the hydrogen flux on the inlet side gauge pressure at 100°C of modified dense-metal Pd-40%Cu membranes and an unmodified pure palladium membrane.

The selectivity of the developed modified membranes was studied through the ratio of passing H<sub>2</sub> to N<sub>2</sub> flows under conditions of a pressure drop in the retentate zone from 0.1 to 0.5 MPa. According to the Figure 11, every investigated membrane showed a fairly high level of selectivity. Pd-Au/M<sub>1</sub> and Pdblack/M<sub>1</sub> films had the highest selectivity up to 4419 at 0.5 MPa. The selectivity of the Pd-Au/M<sub>3</sub> and Pdblack/M<sub>3</sub> films was 3.5 times lower than the selectivity of the Pd-Au/M<sub>1</sub> and Pdblack/M<sub>1</sub> films. Lower selectivity values of membrane Pd-Au/M<sub>3</sub> and Pdblack/M<sub>3</sub> samples indicate the presence of minor defects or a less dense crystal lattice. It should be noted that the selectivity turned out to be quite close for films obtained by the same method, but modified with different coatings. For Pd-Au/M<sub>1</sub> and Pdblack/M<sub>1</sub> films the difference was 1.1 times (4419 and 4055, respectively). For Pd-Au/M<sub>3</sub> and Pdblack/M<sub>3</sub> films the difference was 1.2 times (1503 and 1263, respectively). The experiment was carried out with an increase in pressure up to 0.5 MPa and followed a decrease to started value of 0.1 MPa. At the end of the experiment, the hysteresis dependence was not registered, which confirms the ability of the developed membranes to withstand pressure drops. As the pressure on the inlet side of the membranes increased, a decrease in selectivity was observed, which can be clearly seen at Figure 11. Nevertheless, the numerical selectivity decrease can be considered insignificant. The results make it possible to judge the absence of significant defects in the developed films and the stability of the studied membrane samples to pressure drops.

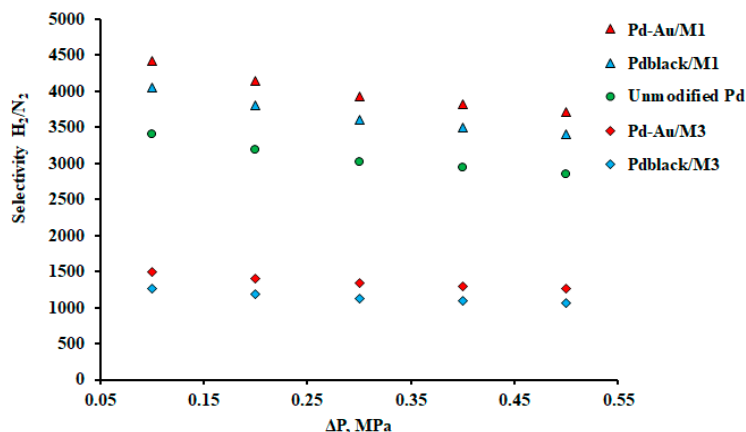


**Figure 11.** Dependence of  $\text{H}_2/\text{N}_2$  selectivity on gauge pressure at the inlet side of Pd-40%Cu membranes and an unmodified pure palladium membrane.

A comparative analysis of the results obtained in this work with the available literature data was carried out to evaluate the efficiency of the developed Pd-Cu membranes (Table 2). However, there are quite a few works with stable and reproducible experimental data on the low-temperature permeability of hydrogen through the palladium phase. And the existing literature reports on obtaining data vary greatly in the quantitative expression of the obtained values. There are practically no works demonstrating the results of experiments on the hydrogen permeability of palladium membranes below 100 °C.

**Table 2.** Hydrogen permeability and  $\text{H}_2/\text{N}_2$  selectivity for the developed membranes and literature analogs.

Membrane	Support	Thickness, $\mu\text{m}$	$J, \text{mmol s}^{-1} \text{m}^{-2}$	Temperature, K	$\Delta p, \text{kPa}$	Selectivity $\text{H}_2/\text{N}_2$	Reference
Pd	YSZ – $\text{Al}_2\text{O}_3$	5	450	623	390	350	[68]
Pd	$\text{Al}_2\text{O}_3$	10	95	573	200	176	[69]
$\text{Pd}_{88}\text{Ag}_{12}$	$\text{Al}_2\text{O}_3$	11	200	623	160	2073	[70]
PdCu/Ta	–	250	5.2	673	100	–	[11]
50 vol. % Pd-GDC	–	282	41	1173	<100	–	[71]
50 vol. % Pd-CZY	–	500	17	1173	<100	–	[72]
50 vol. % Pd-YSZ	–	218	24	1173	<100	–	[73]
$\text{Pd}_{70}\text{Cu}_{30}$	$\text{Al}_2\text{O}_3$	20	105	573	100	1500	[74]
$\text{Pd}_{66}\text{Cu}_{34}$	$\text{Al}_2\text{O}_3$	4	190	783	350	5000	[75]
$\text{Pd}_{47}\text{Cu}_{53}$	$\text{Al}_2\text{O}_3 - \text{ZrO}_2$	3.5	220	573	500	100	[33]
Pd	–	20	0.11	373	500	3399	This work
Pd-Au / M <sub>1</sub>	–	20	59.41	573	100	4419	This work
Pdblack / M <sub>1</sub>	–	20	40.97	573	100	4055	This work
Pd-Au / M <sub>3</sub>	$\text{Al}_2\text{O}_3$	0.3	475.28	573	100	1503	This work
Pdblack / M <sub>3</sub>	$\text{Al}_2\text{O}_3$	0.3	307.29	573	100	1263	This work

#### 4. Conclusions

In this study, a high hydrogen yield was achieved by using thin Pd-40%Cu membranes modified with a pentagonal structured Pd-Au coating. Self-supporting Pd-40%Cu films obtained by melting and rolling and by magnetron sputtering from a Pd-40%Cu target on a substrate were modified in

order to intensify low-temperature hydrogen transport. Classical palladium black and the pentagonal structured Pd-Au particles developed according to controlled synthetic method of were used as surface modifiers. The integration of the developed metal films and surface modifiers made it possible to achieve high catalytic activity and stability in the methanol oxidation reaction. The highest peak current densities were observed up to  $89.47 \text{ mA cm}^{-2}$  for Pd-Au/M<sub>1</sub> films. The obtained values turned out to be 2.2 times higher than ones of Pd<sub>black</sub>/M<sub>1</sub> films ( $40.38 \text{ mA cm}^{-2}$ ) and several tens of times higher than values of unmodified Pd-40%Cu film. Also, Pd-Au/M<sub>1</sub> films had the best resistance to CO poisoning and increased stability ( $2.23 \text{ mA cm}^{-2}$ ). This result may be due to an increased number of localized areas of high-energy surface centers, as well as the presence of a synergistic effect from the secondary metal - gold - in the composition of nanoparticles. The developed membrane materials were studied in the hydrogen transport processes in the temperature range from 25 to 300°C. A significant hydrogen flux increase was experimentally recorded up to  $475.28 \text{ mmol s}^{-1} \text{ m}^{-2}$  and  $59.41 \text{ mmol s}^{-1} \text{ m}^{-2}$  at 300°C for Pd-40%Cu Pd-Au/M<sub>3</sub> and Pd-Au/M<sub>1</sub> membranes respectively. Numerically, the increase was 1.5 times compared to samples of Pd<sub>black</sub>/M<sub>1</sub> and Pd<sub>black</sub>/M<sub>3</sub> membranes. For dense-metal modified membranes, the increase in flux was up to 7 times, compared with a smooth membrane made of pure palladium, and for deposited films, this difference was several tens of times. The achievement of this result is due to an increase in the membrane surface roughness, as well as an increase in the surface active centers number for modifiers of complex geometry, Surface modification has a significant effect, since the hydrogen transfer process is limited by dissociative-associative stages in the selected temperature range. The experiments confirm that the deposition of a pentagonal structured Pd-Au coating on the surface of the developed Pd-40%Cu membranes can significantly reduce surface restrictions by a transition to a diffusion-limited mode. The H<sub>2</sub>/N<sub>2</sub> selectivity for the developed modified membrane materials also showed rather high values and the absence of significant defects in the membranes. The modifying strategy of membrane materials with functional coatings of a fundamentally new complex geometry can shed new light on the development and fabrication of durable and highly selective palladium-based membranes for gas steam reformers.

**Author Contributions:** Conceptualization, I.P.; methodology, I.P.; investigation, I.P., P.P. and G.A.; data curation, P.P. and G.A.; writing—original draft preparation, P.P.; writing—review and editing, I.P.; visualization, G.A.; project administration, I.P.; funding acquisition, I.P.

**Funding:** This research was funded by Russian Science Foundation, grant number 21-72-00045, <https://rscf.ru/project/21-72-00045/>.

**Institutional Review Board Statement:** Not applicable.

**Data Availability Statement:** Not applicable.

**Conflicts of Interest:** The authors declare no conflict of interest.

## References

1. Ongis, M.; Di Marcoberardino, G.; Baiguini, M.; Gallucci, F.; Binotti, M. Optimization of Small-Scale Hydrogen Production with Membrane Reactors. *Membranes* **2023**, *13*, 331. [https://doi.org/10.3390 membranes13030331](https://doi.org/10.3390	membranes13030331)
2. Stenina, I.; Yurova, P.; Achoh, A.; Zabolotsky, V.; Wu, L.; Yaroslavtsev, A. Improvement of Selectivity of RALEX-CM Membranes via Modification by Ceria with a Functionalized Surface. *Polymers* **2023**, *15*, 647. <https://doi.org/10.3390/polym15030647>
3. Falina, I.; Kononenko, N.; Timofeev, S.; Rybalko, M.; Demidenko, K. Nanocomposite Membranes Based on Fluoropolymers for Electrochemical Energy Sources. *Membranes* **2022**, *12*, 935. [https://doi.org/10.3390 membranes12100935](https://doi.org/10.3390	membranes12100935)
4. Butylskii, D.; Troitskiy, V.; Chuprynnina, D.; Kharchenko, I.; Ryzhkov, I.; Apel, P.; Pismenskaya, N.; Nikonenko, V. Selective Separation of Singly Charged Chloride and Dihydrogen Phosphate Anions by Electrobaromembrane Method with Nanoporous Membranes. *Membranes* **2023**, *13*, 455. [https://doi.org/10.3390 membranes13050455](https://doi.org/10.3390	membranes13050455)
5. Achoh, A.R.; Pribytkov, F.B.; But, A.Yu.; Zabolotsky, V.I. Exchange sorption and electrical conductivity of heterogeneous anion-exchange membranes in mixed sodium hydroxide/sodium naphthenate and sodium

sulfate/sodium nitrate nlectrolyte solutions. *Petroleum Chemistry* **2018**, *58*, 1159–1164. <https://doi.org/10.1134/S0965544118130029>

- 6. Shkirskaya, S.A.; Kononenko, N.A.; Timofeev, S.V. Structural and Electrotransport Properties of Perfluorinated Sulfocationic Membranes Modified by Silica and Zirconium Hydrophosphate. *Membranes* **2022**, *12*, 979. <https://doi.org/10.3390/membranes12100979>
- 7. Kozmai, A.E.; Mareev, S.A.; Butylskii, D.Yu.; Ruleva, V.D.; Pismenskaya, N.D.; Nikonenko, V.V. Low-frequency impedance of ion-exchange membrane with electrically heterogeneous surface. *Electrochim. Acta* **2023**, *451*, 142285. <https://doi.org/10.1016/j.electacta.2023.142285>
- 8. Fedotov, A.S.; Tsodikov, M.V.; Yaroslavtsev, A.B. Hydrogen Production in Catalytic Membrane Reactors Based on Porous Ceramic Converters. *Processes* **2022**, *10*, 2060. <https://doi.org/10.3390/pr10102060>
- 9. El-Shafie, M.; Kambra, S.; Hayakawa, Y. Performance evaluation of hydrogen permeation through pd/cu membrane at different plasma system conditions. *S. Afr. J. Chem. Eng.* **2021**, *35*, 118–125. <https://doi.org/10.1016/j.sajce.2020.09.005>
- 10. Petrev, I.; Pushankina, P.; Shostak, N.; Baryshev, M. Gas-Transport Characteristics of PdCu–Nb–PdCu Membranes Modified with Nanostructured Palladium Coating. *Int. J. Mol. Sci.* **2022**, *23*, 228. <https://doi.org/10.3390/ijms23010228>
- 11. Ryu, S.; Badakhsh, A.; Oh, J.G.; Ham, H.C.; Sohn, H.; Yoon, S.P.; Choi, S.H. Experimental and Numerical Study of Pd/Ta and PdCu/Ta Composites for Thermocatalytic Hydrogen Permeation. *Membranes* **2023**, *13*, 23. <https://doi.org/10.3390/membranes13010023>
- 12. Fasolin, S.; Barison, S.; Agresti, F.; Battiston, S.; Fiameni, S.; Isopi, J.; Armelao, L. New Sustainable Multilayered Membranes Based on ZrVTi for Hydrogen Purification. *Membranes* **2022**, *12*, 722. <https://doi.org/10.3390/membranes12070722>
- 13. Yin, Z.; Yang, Z.; Du, M.; Mi, J.; Hao, L.; Tong, Y.; Feng, Y.; Li, S. Effect of annealing process on the hydrogen permeation through Pd–Ru membrane. *J. Membr. Sci.* **2022**, *654*, 120572. <https://doi.org/10.1016/j.memsci.2022.120572>
- 14. Petrev, I.S.; Pushankina, P.D.; Lutsenko, I.S.; Baryshev, M.G. The influence of a crystallographically atypical pentagonal nanostructured coating on the limiting stage of low-temperature hydrogen transport through Pd–Cu membranes. *Doklady Physics* **2021**, *66*, 209–213. <https://doi.org/10.1134/S1028335821080061>
- 15. Nam, S.-E.; Lee, K.-H. Hydrogen separation by Pd alloy composite membranes: introduction of diffusion barrier. *J. Membr. Sci.* **2001**, *192*, 177–185. [https://doi.org/10.1016/S0376-7388\(01\)00499-9](https://doi.org/10.1016/S0376-7388(01)00499-9)
- 16. Nam, S.-E.; Lee, K.-H. Preparation and Characterization of Palladium Alloy Composite Membranes with a Diffusion Barrier for Hydrogen Separation. *Ind. Eng. Chem. Res.* **2005**, *44*, 100–105. <https://doi.org/10.1021/ie040025x>
- 17. Islam, M.S.; Rahman, M.M.; Ilias, S. Characterization of Pd–Cu membranes fabricated by surfactant induced electroless plating (SIEP) for hydrogen separation. *Int. J. Hydrot. Energy* **2012**, *37*, 3477–3490. <https://doi.org/10.1016/j.ijhydene.2011.11.024>
- 18. Kim, D.-W.; Park, Y.J.; Moon, J.-W.; Ryi, S.-K.; Park, J.-S. The effect of Cu reflow on the Pd–Cu–Ni ternary alloy membrane fabrication for infinite hydrogen separation. *Thin Solid Films* **2008**, *516*, 3036–3044. <https://doi.org/10.1016/j.tsf.2007.11.126>
- 19. Knapton, A.G. Palladium alloys for hydrogen diffusion membranes. *Platinum Metals Review* **1977**, *21*, 44–50. <https://citeserx.ist.psu.edu/document?repid=rep1&type=pdf&doi=ad97e592b7172231570bd8b7f71f4c52064c6cf1>
- 20. Pati, S.; Ashok, J.; Dewangan, N.; Chen, T.; Kawi, S. Ultra-thin (~1 μm) Pd–Cu membrane reactor for coupling CO<sub>2</sub> hydrogenation and propane dehydrogenation applications. *J. Membr. Sci.* **2020**, *595*, 117496. <https://doi.org/10.1016/j.memsci.2019.117496>
- 21. Nooijer, N.d.; Arratibel Plazaola, A.; Meléndez Rey, J.; Fernandez, E.; Pacheco Tanaka, D.A.; Sint Annaland, M.v.; Gallucci, F. Long-Term Stability of Thin-Film Pd-Based Supported Membranes. *Processes* **2019**, *7*, 106. <https://doi.org/10.3390/pr7020106>
- 22. Zhao, C.; Liu, Y.; Zhu, H.; Feng, J.; Jiang, H.; An, F.; Jin, Y.; Xu, W.; Yang, Z.; Sun, B. Hydrophobically modified Pd membrane for the efficient purification of hydrogen in light alcohols steam reforming process. *J. Membr. Sci.* **2022**, *647*, 120326. <https://doi.org/10.1016/j.memsci.2022.120326>
- 23. Petrev, I.S.; Lutsenko, I.S.; Pushankina, P.D.; Frolov, V.Yu.; Glazkova, Yu.S.; Malkov, T.I.; Gladkikh, A.M.; Otkidach, M.A.; Sypalo, E.B.; Baryshev, P.M.; Shostak, N.A.; Kopytov, G.F. Hydrogen Transport through Palladium-Coated Niobium Membranes. *Russ. Phys. J.* **2022**, *65*, 312–316. <https://doi.org/10.1007/s11182-022-02637-x>
- 24. Martinez-Diaz, D.; Michienzi, V.; Calles, J.A.; Sanz, R.; Caravella, A.; Alique, D. Versatile and Resistant Electroless Pore-Plated Pd-Membranes for H<sub>2</sub>-Separation: Morphology and Performance of Internal Layers in PSS Tubes. *Membranes* **2022**, *12*, 530. <https://doi.org/10.3390/membranes12050530>

25. Bosko, M.L.; Fontana, A.D.; Tarditi, A.; Cornaglia, L. Advances in hydrogen selective membranes based on palladium ternary alloys. *Int. J. Hydrol. Energy* **2021**, *46*, 15572–15594. <https://doi.org/10.1016/j.ijhydene.2021.02.082>

26. Zhu, K.; Li, X.; Zhang, Y.; Zhao, X.; Liu, Z.; Guo, J. Tailoring the hydrogen transport properties of highly permeable Nb51W5Ti23Ni21 alloy membrane by Pd substitution. *Int. J. Hydrol. Energy* **2022**, *47*, 6734–6744. <https://doi.org/10.1016/j.ijhydene.2021.12.021>

27. Alrashed, F.S.; Paglieri, S.N.; Alismail, Z.S.; Khalaf, H.; Harale, A.; Overbeek, J.P.; van Veen, H.M.; Hakeem, A.S. Steam reforming of simulated pre-reformed naphtha in a PdAu membrane reactor. *Int. J. Hydrol. Energy* **2021**, *46*, 21939–21952. <https://doi.org/10.1016/j.ijhydene.2021.04.020>

28. Sazali, N. A comprehensive review of carbon molecular sieve membranes for hydrogen production and purification. *Int. J. Adv. Manuf. Technol.* **2020**, *107*, 2465–2483. <https://doi.org/10.1007/s00170-020-05196-y>

29. Zhou, Q.; Luo, S.; Zhang, M.; Liao, N. Selective and efficient hydrogen separation of Pd–Au–Ag ternary alloy membrane. *Int. J. Hydrol. Energy* **2022**, *47*, 13054–13061. <https://doi.org/10.1016/j.ijhydene.2022.02.044>

30. Han, Z.; Xu, K.; Liao, N.; Xue, W. Theoretical investigations of permeability and selectivity of Pd–Cu and Pd–Ni membranes for hydrogen separation. *Int. J. Hydrol. Energy* **2021**, *46*, 23715–23722. <https://doi.org/10.1016/j.ijhydene.2021.04.145>

31. Agnolin, S.; Melendez, J.; Di Felice, L.; Gallucci, F. Surface roughness improvement of Hastelloy X tubular filters for H<sub>2</sub> selective supported Pd–Ag alloy membranes preparation. *Int. J. Hydrol. Energy* **2022**, *47*, 28505–28517. <https://doi.org/10.1016/j.ijhydene.2022.06.164>

32. Wei, W.; Liu, L.C.; Gong, H.R.; Song, M.; Chang, M.L.; Chen, D.C. Fundamental mechanism of BCC-FCC phase transition from a constructed PdCu potential through molecular dynamics simulation. *Comput. Mater. Sci.* **2019**, *159*, 440–447. <https://doi.org/10.1016/j.commatsci.2018.12.037>

33. Zhao, C.; Goldbach, A.; Xu, H. Low-temperature stability of body-centered cubic PdCu membranes. *J. Membr. Sci.* **2017**, *542*, 60–67. <https://doi.org/10.1016/j.memsci.2017.07.049>

34. Moon, D.-K.; Han, Y.-J.; Bang, G.; Kim, J.-H.; Lee, C.-H. Palladium-copper membrane modules for hydrogen separation at elevated temperature and pressure. *Korean J. Chem. Eng.* **2019**, *36*, 563–572. <https://doi.org/10.1007/s11814-019-0237-7>

35. Howard, B.H.; Killmeyer, R.P.; Rothenberger, K.S.; Cugini, A.V.; Morreale, B.D.; Enick, R.M.; Bustamante, F. Hydrogen permeance of palladium–copper alloy membranes over a wide range of temperatures and pressures. *J. Membr. Sci.* **2004**, *241*, 207–218. <https://doi.org/10.1016/j.memsci.2004.04.031>

36. Nayebossadri, S.; Speight, J.; Book, D. Effects of low Ag additions on the hydrogen permeability of Pd–Cu–Ag hydrogen separation membranes. *J. Membr. Sci.* **2014**, *451*, 216–225. <https://doi.org/10.1016/j.memsci.2013.10.002>

37. Martin, M.H.; Galipaud, J.; Tranchot, A.; Roué, L.; Guay, D. Measurements of hydrogen solubility in CuxPd100–x thin films. *Electrochim. Acta* **2013**, *90*, 615–622. <https://doi.org/10.1016/j.electacta.2012.10.140>

38. Yuan, L.; Goldbach, A.; Xu, H. Segregation and H<sub>2</sub> Transport Rate Control in Body-Centered Cubic PdCu Membranes. *J. Phys. Chem. B* **2007**, *111*, *37*, 10952–10958. <https://doi.org/10.1021/jp073807n>

39. Gao, M.C.; Ouyang, L.; Doğan, Ö.N. First principles screening of B<sub>2</sub> stabilizers in CuPd-based hydrogen separation membranes: (1) Substitution for Pd. *J. Alloys Compd.* **2013**, *574*, 368–376. <https://doi.org/10.1016/j.jallcom.2013.05.126>

40. Yuan, L.; Goldbach, A.; Xu, H. Permeation Hysteresis in PdCu Membranes. *J. Phys. Chem. B* **2008**, *112*, 12692–12695. <https://doi.org/10.1021/jp8049119>

41. Opalka, S.M.; Huang, W.; Wang, D.; Flanagan, T.B.; Løvvik, O.M.; Emerson, S.C.; She, Y.; Vanderspurt, T.H. Hydrogen interactions with the PdCu ordered B<sub>2</sub> alloy. *J. Alloys Compd.* **2007**, *583*–587. <https://doi.org/10.1016/j.jallcom.2007.01.130>

42. Shinoda, Y.; Takeuchi, M.; Dezawa, N.; Komo, Y.; Harada, T.; Takasu, H.; Kato, Y. Development of a H<sub>2</sub>-permeable Pd60Cu40-based composite membrane using a reverse build-up method. *Int. J. Hydrol. Energy* **2021**, *46*, 36291–36300. <https://doi.org/10.1016/j.ijhydene.2021.08.127>

43. Roa, F.; Block, M.J.; Way, J.D. The influence of alloy composition on the H<sub>2</sub> flux of composite Pd–Cu membranes. *Desalination* **2002**, *147*, 411–416. [https://doi.org/10.1016/S0011-9164\(02\)00636-7](https://doi.org/10.1016/S0011-9164(02)00636-7)

44. Yang, Y.; Li, X.; Liang, X.; Chen, R.; Guo, J.; Fu, H.; Liu, D. A two-step electroless plating method for Pd composite membranes with enhanced hydrogen selectivity and superior high-temperature stability. *J. Environ. Chem. Eng.* **2022**, *10*, 108477. <https://doi.org/10.1016/j.jece.2022.108477>

45. Martinez-Diaz, D.; Alique, D.; Calles, J.A.; Sanz, R. Pd-thickness reduction in electroless pore-plated membranes by using doped-ceria as interlayer. *Int. J. Hydrol. Energy* **2020**, *45*, 7278–7289. <https://doi.org/10.1016/j.ijhydene.2019.10.140>

46. Melendez, J.; Fernandez, E.; Gallucci, F.; van Sint Annaland, M.; Arias, P.L.; Pacheco Tanaka, D.A. Preparation and characterization of ceramic supported ultra-thin (~1 μm) Pd–Ag membranes. *J. Membr. Sci.* **2017**, *528*, 12–23. <https://doi.org/10.1016/j.memsci.2017.01.011>

47. Gao, H.; Lin, J.Y.S.; Li, Y.; Zhang, B. Electroless plating synthesis, characterization and permeation properties of Pd–Cu membranes supported on ZrO<sub>2</sub> modified porous stainless steel. *J. Membr. Sci.* **2005**, *265*, 142–152. <https://doi.org/10.1016/j.memsci.2005.04.050>

48. Dube, S.; Gorimbo, J.; Moyo, M.; Okoye-Chine, C.G.; Liu, X. Synthesis and application of Ni-based membranes in hydrogen separation and purification systems: A review. *J. Environ. Chem. Eng.* **2023**, *11*, 109194. <https://doi.org/10.1016/j.jece.2022.109194>

49. Hoang, H.T.; Tong, H.D.; Gielens, F.C.; Jansen, H.V.; Elwenspoek, M.C. Fabrication and characterization of dual sputtered Pd–Cu alloy films for hydrogen separation membranes. *Mater. Lett.* **2004**, *58*, 525–528. [https://doi.org/10.1016/S0167-577X\(03\)00539-1](https://doi.org/10.1016/S0167-577X(03)00539-1)

50. Ryi, S.-K.; Park, J.-S.; Kim, S.-H.; Cho, S.-H.; Kim, D.-W.; Um, K.-Y. Characterization of Pd–Cu–Ni ternary alloy membrane prepared by magnetron sputtering and Cu-reflow on porous nickel support for hydrogen separation. *Sep. Purif. Technol.* **2006**, *50*, 82–91. <https://doi.org/10.1016/j.seppur.2005.11.024>

51. Jokar, S.M.; Farokhnia, A.; Tavakolian, M.; Pejman, M.; Parvasi, P.; Javanmardi, J.; Zare, F.; Gonçalves, M.C.; Basile, A. The recent areas of applicability of palladium based membrane technologies for hydrogen production from methane and natural gas: A review. *Int. J. Hydrog. Energy* **2023**, *48*, 6451–6476. <https://doi.org/10.1016/j.ijhydene.2022.05.296>

52. Petriev, I.; Pushankina, P.; Bolotin, S.; Lutsenko, I.; Kukueva, E.; Baryshev, M. The influence of modifying nanoflower and nanostar type Pd coatings on low temperature hydrogen permeability through Pd-containing membranes. *J. Membr. Sci.* **2021**, *620*, 118894. <https://doi.org/10.1016/j.memsci.2020.118894>

53. Vicinanza, N.; Svenum, I.-H.; Peters, T.; Bredesen, R.; Venvik, H. New Insight to the Effects of Heat Treatment in Air on the Permeation Properties of Thin Pd77%Ag23% Membranes. *Membranes* **2018**, *8*, 92. <https://doi.org/10.3390/membranes8040092>

54. Vielstich, W. Brennstoffelemente. Moderne Verfahren zur elektrochemischen Energiegewinnung; Verlag Chemie: Weinheim, Deutschland, 1965; pp. 388.

55. Basov, A.; Dzhimak, S.; Sokolov, M.; Malyshko, V.; Moiseev, A.; Butina, E.; Elkina, A.; Baryshev, M. Changes in Number and Antibacterial Activity of Silver Nanoparticles on the Surface of Suture Materials during Cyclic Freezing. *Nanomaterials* **2022**, *12*, 1164. <https://doi.org/10.3390/nano12071164>

56. Petriev, I.; Pushankina, P.; Glazkova, Y.; Andreev, G.; Baryshev, M. Investigation of the Dependence of Electrocatalytic Activity of Copper and Palladium Nanoparticles on Morphology and Shape Formation. *Coatings* **2023**, *13*, 621. <https://doi.org/10.3390/coatings13030621>

57. Pushankina, P.; Baryshev, M.; Petriev, I. Synthesis and Study of Palladium Mono- and Bimetallic (with Ag and Pt) Nanoparticles in Catalytic and Membrane Hydrogen Processes. *Nanomaterials* **2022**, *12*, 4178. <https://doi.org/10.3390/nano12234178>

58. Petriev, I.S.; Pushankina, P.D.; Lutsenko, I.S.; Baryshev, M.G. Anomalous Kinetic Characteristics of Hydrogen Transport through Pd–Cu Membranes Modified by Pentatwinned Flower-Shaped Palladium Nanocrystallites with High-Index Facets. *Tech. Phys. Lett.* **2021**, *47*, 803–806. <https://doi.org/10.1134/S1063785021080216>

59. Petriev, I.; Pushankina, P.; Lutsenko, I.; Shostak, N.; Baryshev, M. Synthesis, Electrocatalytic and Gas Transport Characteristics of Pentagonally Structured Star-Shaped Nanocrystallites of Pd–Ag. *Nanomaterials* **2020**, *10*, 2081. <https://doi.org/10.3390/nano10102081>

60. Wang, L.; Zhai, J.-J.; Jiang, K.; Wang, J.-Q.; Cai, W.-B. Pd–Cu/C electrocatalysts synthesized by one-pot polyol reduction toward formic acid oxidation: Structural characterization and electrocatalytic performance. *Int. J. Hydrog. Energy* **2015**, *40*, 1726–1734. <https://doi.org/10.1016/j.ijhydene.2014.11.128>

61. Xiong, Y.; Ye, W.; Chen, W.; Wu, Y.; Xu, Q.; Yan, Y.; Zhang, H.; Wu, J.; Yang, D. PdCu alloy nanodendrites with tunable composition as highly active electrocatalysts for methanol oxidation. *RSC Adv.* **2017**, *7*, 5800–5806. <https://doi.org/10.1039/C6RA25900F>

62. Shan, S.; Petkov, V.; Prasai, B.; Wu, J.; Joseph, P.; Skeete, Z.; Kim, E.; Mott, D.; Malis, O.; Luoa, J.; Zhong, C.-J. Catalytic activity of bimetallic catalysts highly sensitive to the atomic composition and phase structure at the nanoscale. *Nanoscale* **2015**, *7*, 18936–18948. <https://doi.org/10.1039/C5NR04535E>

63. Al-Mufachi, N.A.; Nayebossadri, S.; Speight, J.D.; Bujalski, W.; Steinberger-Wilckens, R.; Book, D. Effects of thin film Pd deposition on the hydrogen permeability of Pd60Cu40 wt% alloy membranes. *J. Membr. Sci.* **2015**, *493*, 580–588. <https://doi.org/10.1016/j.memsci.2015.07.015>

64. Yeon, S.; Lee, S.J.; Chinnadurai, D.; Yu, Y.; Lee, Y.W.; Choi, M.Y. Rapid alloying of Au–Pd nanospheres by a facile pulsed laser technique: Insights into a molar-dependent electrocatalytic methanol oxidation reaction. *J. Alloys Compd.* **2022**, *891*, 162011. <https://doi.org/10.1016/j.jallcom.2021.162011>

65. Woo, S.; Lee, J.; Park, S.-K.; Kim, H.; Chung, T. D.; Piao, Y. Electrochemical codeposition of Pt/graphene catalyst for improved methanol oxidation. *Current Applied Physics* **2015**, *15*, 219–225. <https://doi.org/10.1016/j.cap.2014.12.022>

66. Huang, W.; Kang, X.; Xu, C.; Zhou, J.; Deng, J.; Li, Y.; Cheng, S. 2D PdAg Alloy Nanodendrites for Enhanced Ethanol Electrooxidation. *Adv. Mater.* **2018**, *30*, 1706962. <https://doi.org/10.1002/adma.201706962>

67. Yin, Z.; Chi, M.; Zhu, Q.; Ma, D.; Sune, J.; Bao, X. Supported bimetallic PdAu nanoparticles with superior electrocatalytic activity towards methanol oxidation. *J. Mater. Chem. A* **2013**, *1*, 9157–9163. <https://doi.org/10.1039/C3TA11592E>
68. Pacheco Tanaka, D.A.; Llosa Tanco, M.A.; Okazaki, J.; Wakui, Y.; Mizukami, F.; Suzuki, T.M. Preparation of “pore-fill” type Pd-YSZ- $\gamma$ -Al<sub>2</sub>O<sub>3</sub> composite membrane supported on  $\alpha$ -Al<sub>2</sub>O<sub>3</sub> tube for hydrogen separation. *J. Membr. Sci.* **2008**, *320*, 436–441. <https://doi.org/10.1016/j.memsci.2008.04.044>
69. Arratibel, A.; Astobidea, U.; Pacheco Tanaka, D.A.; van Sint Annaland, M.; Gallucci, F. N<sub>2</sub>, He and CO<sub>2</sub> diffusion mechanism through nanoporous YSZ/ $\gamma$ -Al<sub>2</sub>O<sub>3</sub> layers and their use in a pore-filled membrane for hydrogen membrane reactors. *Int. J. Hydrot. Energy* **2016**, *41*, 8732–8744. <https://doi.org/10.1016/j.ijhydene.2015.11.152>
70. Nair, B.K.R.; Choi, J.; Harold, M.P. Electroless plating and permeation features of Pd and Pd/Ag hollow fiber composite membranes. *J. Membr. Sci.* **2007**, *288*, 67–84. <https://doi.org/10.1016/j.memsci.2006.11.006>
71. Balachandran, U. (Balu); Lee, T.H.; Park, C.Y.; Emerson, J.E.; Picciolo, J.J.; Dorris, S.E. Dense cermet membranes for hydrogen separation. *Sep. Purif. Technol.* **2014**, *121*, 54–59. <https://doi.org/10.1016/j.seppur.2013.10.001>
72. Sato, K.; Nishioka, M.; Higashi, H.; Inoue, T.; Hasegawa, Y.; Wakui, Y.; Suzuki, T.M.; Hamakawa, S. Influence of CO<sub>2</sub> and H<sub>2</sub>O on the separation of hydrogen over two types of Pd membranes: Thin metal membrane and pore-filling-type membrane. *J. Membr. Sci.* **2012**, *415–416*, 85–92. <https://doi.org/10.1016/j.memsci.2012.04.053>
73. Nair, B.K.R.; Harold, M.P. Pd encapsulated and nanopore hollow fiber membranes: Synthesis and permeation studies. *J. Membr. Sci.* **2007**, *290*, 182–195. <https://doi.org/10.1016/j.memsci.2006.12.028>
74. Iulianelli, A.; Ghasemzadeh, K.; Marelli, M.; Evangelisti, C. A supported Pd-Cu/Al<sub>2</sub>O<sub>3</sub> membrane from solvated metal atoms for hydrogen separation/purification. *Fuel Process. Technol.* **2019**, *195*, 106141. <https://doi.org/10.1016/j.fuproc.2019.106141>
75. Pan, X.; Kilgus, M.; Goldbach, A. Low-temperature H<sub>2</sub> and N<sub>2</sub> transport through thin Pd<sub>66</sub>Cu<sub>34</sub>H<sub>x</sub> layers. *Catal. Today* **2005**, *104*, 225–230. <https://doi.org/10.1016/j.cattod.2005.03.049>

**Disclaimer/Publisher’s Note:** The statements, opinions and data contained in all publications are solely those of the individual author(s) and contributor(s) and not of MDPI and/or the editor(s). MDPI and/or the editor(s) disclaim responsibility for any injury to people or property resulting from any ideas, methods, instructions or products referred to in the content.